

EXPERIMENTAL STUDY OF THE STRESS PATHS INFLUENCE ON MONOPHASIC PERMEABILITY EVOLUTION

J-P. Sarda, F.M.R. Ferfera¹, O. Vincké, M. Boutéca and P. Longuemare

Institut Français du Pétrole 1 & 4 avenue de Bois-Préau 92852 Rueil Malmaison - France

ABSTRACT

Permeability changes have been measured during triaxial tests performed on two sets of Vosges sandstone core samples characterized by their mean porosity : about 20% for one set, 17% for the other one. Several loading paths have been investigated, the samples being loaded up to rupture : constant confining pressure, constant mean stress, proportional loading. Attention was paid to the levels of confining pressure and pore pressure in order to emphasize the possible influence of the stress deviator q . The results are analyzed in order to evidence this influence and the influence of the effective mean stress p' (total mean stress minus pore pressure). It is shown that a criterion can be defined in the $(p'-q)$ plot for the permeability evolution. Inside the domain defined by the criterion, the permeability change is nil or small whatever the loading path is. Outside this domain, the permeability change appears to depend on the initial porosity. Indeed the permeability of 20% porosity sandstones steadily decreases, and the permeability reduction rate can be determined for a given stress path and a given level of the stress deviator. At the contrary outside the domain of low permeability variation, the permeability of the 17% porosity sandstones increases and the threshold for permeability increase appears to coincide with the threshold of mechanical damage.

1- INTRODUCTION

During the primary production of hydrocarbons the main mechanism is the fluid expansion resulting from the reservoir pressure decrease. The production thus induces a depletion that in turn induces variations of the in-situ stresses. These stress variations finally induce strains. Most of the time the rock is assumed to deform uniaxially - the so-called oedometric case. However in situ measurements (*Rhett and Teufel*) have shown that the ratio K of the

¹ Now with Sonatrach Company, Algeria.

effective horizontal stress variation ($\Delta\sigma'_h$) and to the effective vertical stress variation ($\Delta\sigma'_v$) is constant. As a consequence the deviator stress change ($\Delta q = \Delta\sigma'_v - \Delta\sigma'_h$) increases while the pore pressure decreases. For example, in the elastic domain (Δp_p negative, b Biot coefficient) :

$$\Delta q = -b(1-K)\Delta p_p$$

The reservoir depletion as well induces changes of the mechanical parameters and of the petrophysical characteristics of the rock. The permeability can thus drastically drop, reducing the well productivity and the economics of the well production can even be endangered. However, at the contrary, examples of permeability increase have been reported from laboratory tests (*Rhett and Teufel, Zhu and Wong*).

Since *Fatt & Davis* pioneering works (1952), permeability variation due to the reservoir production has been much studied (*David, Wilhelmi, Gray, Holt, Morita, Rhett, Teufe, Zhu and Wong*). Figure 1 presents the volume deformation of a rock as a function of a compression loading of any kind. This volume deformation can be described using several possible mechanisms. The first mechanism, corresponding to the initial non linear part of the curve, would be the closure of preexisting cracks. The second one corresponds to a linear phase in a sandstone such as the Vosges sandstone and would correspond to an elastic compression of the rock. Other mechanisms would explain the third, non linear phase, of the curve : grain sliding, pore collapse, grain crushing would lead to volume decrease whereas the propagation of existing cracks would lead to volume increase (i.e. dilatancy).

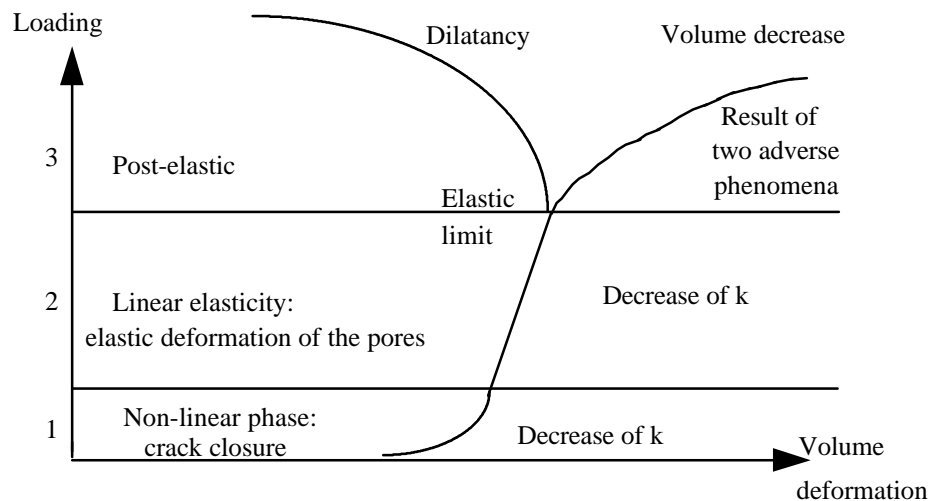


Figure 1 : Loading, volume deformation and permeability : starting point.

From a literature survey it appears that this diagram is frequently used as a physical and mechanical basis to interpret the evolution of permeability : permeability decrease associated

with the lower non-linear part of the curve (closure of cracks), permeability decrease associated with the linear part (elastic compression), permeability decrease or increase associated with the upper non-linear part of this curve. In fact the limit between phase 2 and 3 defines a damage threshold, in the sense that, over this limit, either the Young modulus or the shear modulus starts decreasing. So this diagram means that a new trend in permeability evolution should be observed over this damage threshold.

In order to better understand these phenomena, and particularly the role of the stress deviator during the post-elastic phase, strains and permeability changes have been simultaneously measured during triaxial loading experiments performed on a porous sandstone. Several loading paths have been investigated together with several pore pressure and confining pressure levels. The results are analyzed in order to evidence the influence of the effective mean stress ($p' = (\mathbf{s}_v + 2\mathbf{s}_h)/3 - P_p$) and the influence of the stress deviator q ($q = \mathbf{s}_v - \mathbf{s}_h$). P_p stands for the pore pressure.

2 - EXPERIMENTAL PROCEDURES

a) Rock samples : petrophysical properties, preparation : This research is focused on porous sandstones, which constitute 80% of the hydrocarbons reservoirs. We selected the Vosges sandstone (« grès des Vosges »). Its matrix typical composition is : quartz 80%, feldspars 15%, clays and micas 5%. The core samples (40 mm diameter, 80 mm height) were cored in two blocks, perpendicular to the bedding plane. After surfacing and scanning in an X-Ray computed tomography device in order to spot any petrographic defect (crack for instance) that could hamper permeability and strain measurements, matrix density, elastic wave velocities and porosity were measured. Porosities appeared to be very homogeneous in both blocks but (unexpectedly) different : mean porosity 19.5% in one block, 17% in the other one. Later on, permeability measurements showed that the corresponding permeabilities were very different : 320 md to 460md in the first block, less than 1md in the second one. After measurement of the basic petrophysical properties, strain gauges (3 horizontal and 3 vertical gauges) are glued on the selected samples which are finally coated with a rubber sleeve.

b) Permeability and rock mechanics measurements : In our experiments we used the classical steady flow method. The differential pressure between the inlet and the outlet of the core is measured under constant flow rate (Q) conditions. Given the core inlet section S, the core length L and the fluid dynamic viscosity μ for a given temperature and a given fluid pressure, the permeability can be determined from Darcy's law (Darcy) : $k = -\frac{mQL}{S\Delta p}$.

Oil was used as the saturating fluid. This minimizes physico-chemical interactions between the saturating fluid and the rock. As the oil viscosity can depend on pressure and

temperature, it was necessary to characterize the corresponding viscosity changes. Viscosity changes have been plotted in Figure 2 for the fluid used in our experiments. Since temperature is roughly constant in the laboratory, the most important parameter was the pressure. In our experiments, the pore pressure has been changed in the range [5-35 MPa].

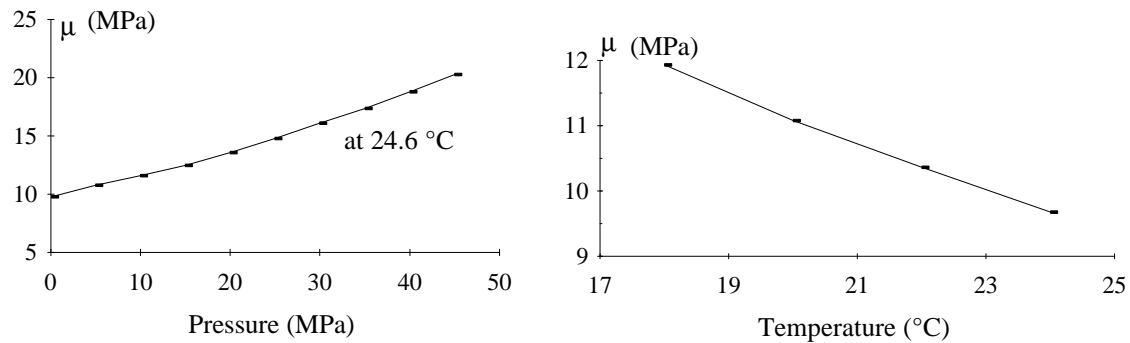


Figure 2 : Influence of pressure and temperature on oil dynamic viscosity

The experimental set-up consists of 3 parts (see Figure 3) : a) a triaxial cell ; b) a pressure circuit including a differential pressure transducer, tubings and 3 pumps allowing pressure or flow regulation ; c) an automatic system for stress path control and data acquisition. This set-up allows pore and confining pressure monitoring, as well as strain and permeability measurements.

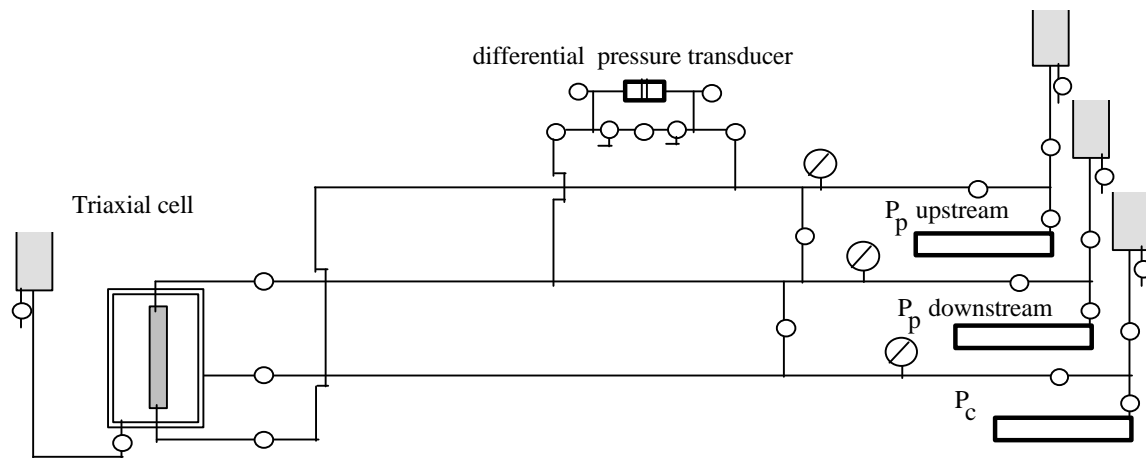


Figure 3 : Experimental set-up

The core sample is set vertically in the triaxial cell. Porous plates are set on both ends to ensure a better flow distribution. The sample is then saturated using the hydraulic device previously described. The vertical loading is mechanically applied and automatically controlled. The confining pressure is applied and controlled through one of the 3 pumps. In

parallel, pore pressure is applied and controlled through one of the 2 remaining pumps up to the selected pressure level. The stress increase rate is 0.1 MPa/mn for isotropic loading and 0.5 MPa/mn otherwise. After stabilizing, two permeability measurements are made. First a flow rate is set at one face of the sample while maintaining the pressure constant at the other face : permeability is thus determined along one direction. Then the flow rate is inverted and permeability is thus determined along the opposite direction. The injection flow rate is in the range of 0.5 cm³/mn to a few cm³/mn, the injection time was set at a few minutes. The recorded permeability value is the mean value of these 2 measurements. This procedure avoids plugging of the pore throats by small particles (*Khilar and Fogler*) and allows duplicating each measurement under identical conditions. The applicability of Darcy's law has been thoroughly checked during the tests. Repeated measurements under similar conditions led to a variation of 5% which represents the experimental error. Finally we compared permeability measurements with gas (air) and with oil for 2 samples. The obtained values are 800 mD for the measurements performed with air and 650 mD for the measurements performed with oil.

c) Loading paths : The experimental parameters that control permeability and strains are the vertical stress, the confining pressure and the pore pressure. In order to analyze the results from a mechanical viewpoint, these parameters have been varied according to given loading stress paths. Four loading paths have been investigated : a) isotropic loading - this phase is performed before any other loading path ; b) vertical loading with constant confining pressure at different pore pressure levels (VL) ; c) proportional loading with constant pore pressure equal to 5 MPa (PRL)- vertical and horizontal stress loading are proportional, the effective stress ratio $\Delta\sigma'_h / \Delta\sigma'_v = K$ has been set equal to 0.1 and 0.2 ; d) constant mean stress $p = (\sigma_v + 2 \sigma_h) / 3$, with a constant pore pressure equal to 5 Mpa (CMS). As an example, table 1 summarizes the tests performed on the 20% porosity samples.

Table 1 : Vertical loading (VL) tests performed on the 20% porosity samples

confining pressure	pore pressure
Pc= 10, 20, 30, 40 MPa	Pp= 5 MPa.
Pc= 20, 30 , 40 Mpa	Pp= 15 MPa.
Pc= 30 , 40 Mpa	Pp= 25 MPa
Pc= 40 MPa	Pp= 35 MPa

3 - UPPER POROSITY SAMPLES/RESULTS AND DISCUSSION

A full report on the petrophysical and mechanical behavior of the 19.5% porosity samples is given in Ferfera (*Ferfera*).

a) Homogeneity of the sampling : Measurements performed on each core under identical conditions - $P_c = 10$ MPa, $P_p = 5$ MPa - lead to very similar values of permeability. About 80% of the tested samples have a permeability in the range of 320 - 460 mD. These homogeneous values stem from the initial choice of the rock together with the screening technique based on CT-Scan results. This homogeneity facilitated the comparison between experiments and hence the analysis.

b) Isotropic loading : The numerous measurements performed during the isotropic phase that precedes the deviatoric phase allowed calculation of David's (*David*) γ coefficient. This coefficient corresponds to the slope of the $\ln k/k_0$ v.s. $p' - p'_0$ plot. k_0 is the initial permeability under isotropic conditions, p' is the Terzaghi effective mean stress (isotropic stress minus pore pressure) and p'_0 its initial value. The mean value obtained for γ ($\gamma = 0.004$ MPa⁻¹, Figure 4) is in the range of values obtained by Yale (*Yale*) (0.0014 - 0.02 MPa⁻¹) for sandstones having similar porosities.

c) Vertical loading : In Figure 5, results obtained for vertical compression tests (VL) with a constant pore pressure of 5 MPa are sorted according to the confining pressure applied. The higher the confining stress, the higher is the final decrease of permeability. These results are in agreement with previous results obtained by Teufel (*Teufel*) with pre-fractured Coconino sandstone and with results obtained by Krishnan et al. (*Krishnan et al*) with Alter sandstone having a weak cementation.

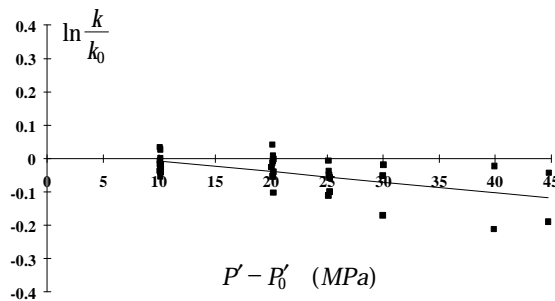


Figure 4 : k measurement under isotropic stress at constant P_p

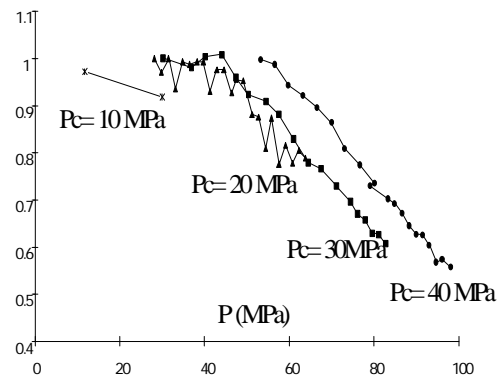


Figure 5 : k/k_0 variation at constant confining stress P_c and $P_p = 5$ MPa

Plotting the same results as a function of the deviatoric stress leads to a single curve thus evidencing a $k/k_0 = f(q)$ curve (figure 6). Further results obtained for a 15 MPa pore pressure are in agreement with these ones thus confirming the $k/k_0 = f(q)$ trend. However a more careful examination of the 2 sets of results, by plotting both of them in the same plot, reveals a slight difference (figure 7). The permeability decrease for a 5 MPa pore pressure is slightly less than the one obtained for a 15 MPa pore pressure. In fact, when plotting all our results in this plot, the obtained curves range within these 2 sets. Hence the

deviatoric stress has a predominant role and leads to a good estimate of the permeability variation but the pore pressure cannot be neglected nor the mean effective stress.

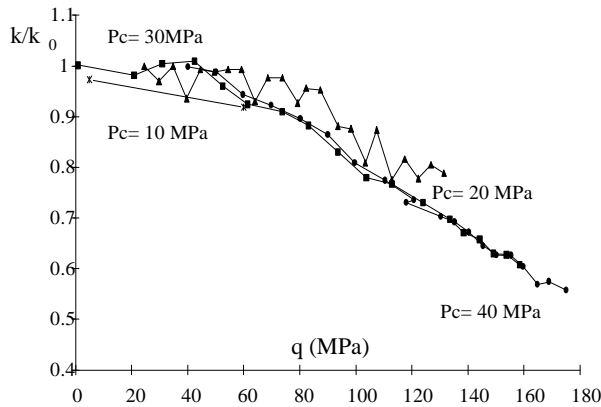


Figure 7 : Vertical loading at constant confining stress and $P_p = 5$ MPa

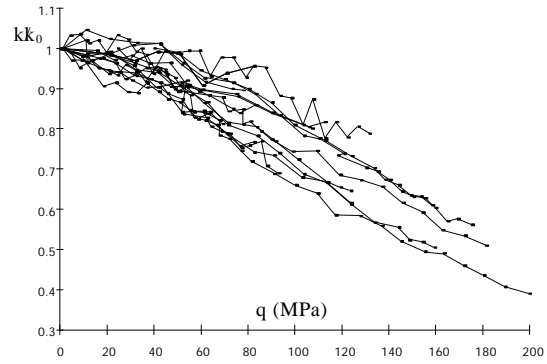


Figure 8 : Permeability of the sandstone along various stress paths (VL, PRL and CMS)

In any case the evolution of the permeability is always characterized by a 2 steps evolution. In the first step the permeability decreases slowly - less than 6%. It then decreases after a threshold more rapidly, the permeability reduction being as high as 60% in some cases - proportional loading with $K=0.1$. The permeability changes thresholds of all the experiments have been plotted in a p' - q plot (Figure 8). A criterion for the permeability behavior is thus evidenced. Within the domain limited by the criterion, the permeability variation is low or even nil. Outside the domain, a significant variation is observed. In the same p' - q plot we plotted the damage criterion and the failure envelope. The damage threshold is defined as the point where Young's modulus and the shear modulus decrease. It can be observed in Figure 8 that the permeability criterion is lower than the damage criterion. Both tend towards similar values when the mean stress decreases. The permeability reduction rate (r_k) is constant after the permeability threshold. Analyzing the results indicate that this rate is always the same for a given stress path and does not depend on the level of the stresses.

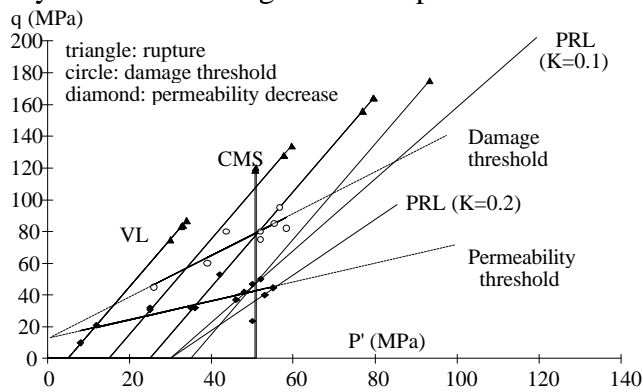


Figure 8 : Mechanical and petrophysical thresholds for various loading paths.

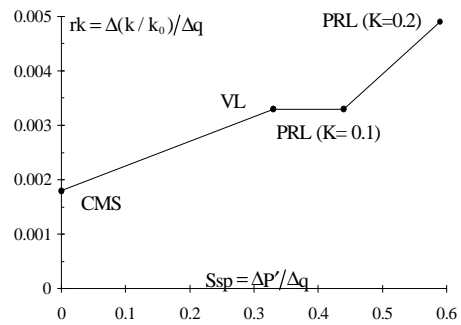


Figure 9 : Influence of the stress path on the permeability reduction rate.

In Figure 9 we plotted r_k as a function of the slope s_{sp} that characterizes the stress path in the p' - q plot. It shows that the permeability reduction rate increases when the stress path moves towards the isotropic loading. As a matter of fact, when the stress path is dominated by the increase of the deviator, the dilatancy tends to counter-balance the permeability reduction. These results are in agreement with results obtained by Rhett and Teufel (*Rhett et Teufel*) and validate the hypothesis made by Krishnan (*Krishnan et al*), who assumed "path dependency of the material under permeability measurement".

4 - LOWER POROSITY SAMPLES : RESULTS AND DISCUSSION

The average porosity of these samples is 17%. Figure 10 shows a typical stress-strain curve, this one being obtained for a 50 Mpa confining stress. The deviator stress q is plotted vs three deformations : on the right the vertical deformation, on the left the horizontal and volume deformations. Figure 11 presents the permeability evolution as a function of the deviator stress. After an initial decrease (closure of microcracks ?), the permeability shows a slight decrease up to 120 Mpa, then increases, finally increases faster in the 180-220 Mpa range.

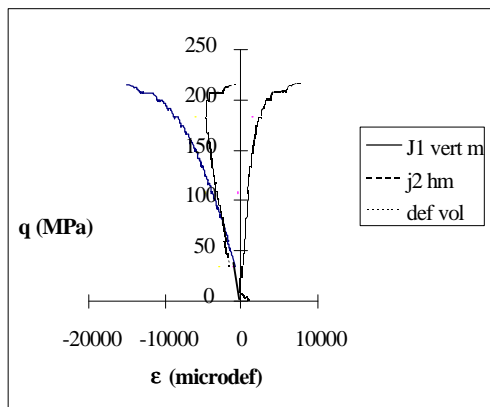


Figure 10 : deviator stress vs vertical, horizontal and volume deformations

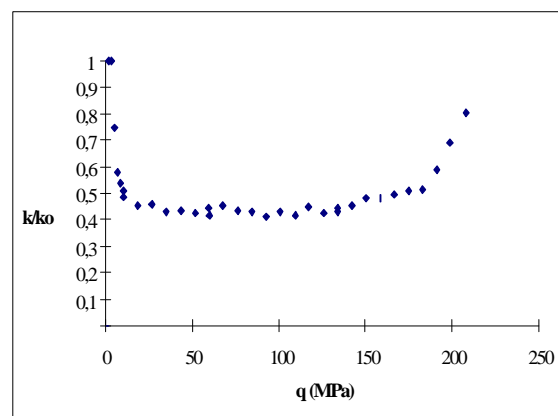


Figure 11 : permeability variation (k/k_0) vs deviator stress. Confining pressure 50 Mpa

The results of three triaxial tests are presented in the (p' , q) plane on Figure 12. These tests correspond to 3 different confining stresses - 10 Mpa, 30 Mpa, 50 Mpa - et to the same pore pressure - 5 Mpa. The loading path shows first the isotropic loading phase, then the deviatoric loading phase. The upper line in the diagram represents the rupture limit of the samples. Inside this limit, rectangles indicate the q value over which permeability increases, whereas the circles indicate, using the volume deformation, the q value over which mechanical damage appears. In the second test (confining stress 30 Mpa) these two symbols coincide. Two dotted lines show the damage criterion (small dots) and the permeability increase criterion (larger dots). Two conclusions appear very clearly. First there is a permeability increase, beginning very early (55% of the rupture stress on Figure 11), which

did not exist in the tests performed on the other set of samples (19.5% average porosity). Secondly this permeability increase coincides (given the experimental uncertainties) with the

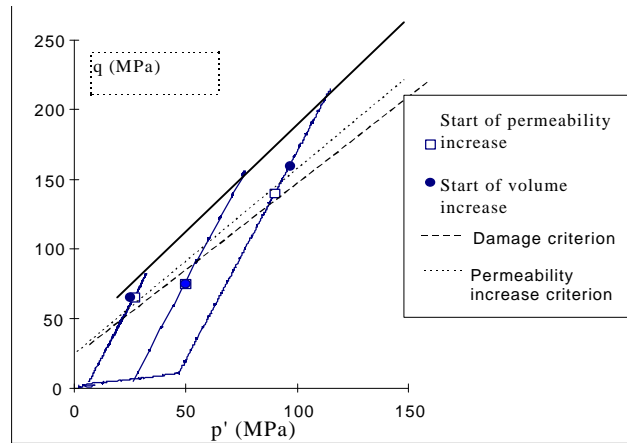


Figure 12 : comparison of damage criterion and k increase criterion for three triaxial tests.

mechanical damage threshold. It can be suggested that, in this low permeability rock, the onset of fissure propagation plays a major role in the evolution of permeability.

5 - CONCLUSIONS

1. We evidenced a criterion in the p' - q plot for permeability changes in a sandstone. Within the domain limited by the criterion, the permeability variation is low or even nil. Outside the domain, a significant variation is observed.
2. The permeability variation outside the domain limited by the criterion depends on the initial petrophysical properties of the sandstone. At this stage of the mechanical interpretation we make a distinction between upper porosity samples (19.5%) and lower porosity samples (17%).
3. In upper porosity sandstones :
 - The permeability criterion stays below the damage threshold.
 - Outside the domain defined by the permeability criterion, permeability decreases. A unique permeability reduction rate is obtained for a given stress path. The more deviatoric the stress path, the lower is the reduction of the permeability.
4. In lower porosity sandstones :
 - The permeability criterion coincides with the mechanical damage threshold.
 - Outside the domain defined by the permeability criterion, permeability increases.

Further tests are planned to characterize this permeability increase.
5. The phenomenon of permeability decrease in higher porosity samples is thought to be related with micro slidings and eventually production of rock powder. Permeability increase in lower porosity samples would coincide with opening and progressing microcracks.

REFERENCES

- Bernabe, Y., Brace, W.F. and Evans, B. (1982). Permeability, porosity and pore geometry of hot-pressed calcite. *Mechanics of Materials* 1, 173-183.
- David, C., Wong, T.F., Zhu, W. and Zhang J. (1993). Laboratory measurements of compaction-induced permeability change in porous rocks: implications for the generation and maintenance of pore pressure excess in the rock. Submitted to *PAGEOPH*.
- Fatt, I. and Davis, D.H. (1952). Reduction in permeability with overburden pressure. *Petroleum Transactions, AIME*, vol.195, 329.
- Ferfera, F. (1997). Influence du champ de contrainte sur l'évolution de la perméabilité monophasique d'un grès. *Ecole Centrale de Paris Thesis*.
- Gray, D.H., Fatt, I. and Bergamini, G. (1963). The effect of stress on permeability of sandstone cores. *SPEJ*, June, 95-100.
- Holt, R.M. (1990). Permeability reduction induced by a nonhydrostatic stress field. *SPE Formation Evaluation*, Dec, 444-448.
- Khilar, C. and Fogler, H.C. (1983). Water sensitivity of sandstones. *SPE/AIME*, Feb., 55-64.
- Krishnan, G.R., Zaman, M.M. and Roegiers, J.-C. (1996). Permeability measurements under different stress paths for a weakly cemented sandstone. *Rock Mechanics, Aubertin, Hassani & Mitri eds.*, Balkema, Rotterdam, 1011-1017.
- Morita, N., Gray, K., Srouji F.A.A. and Jogi. P.N. (1984). Rock property changes during reservoir compaction, *SPE/AME*, Sept., Paper 13099.
- Read, M.D., Meredith, P.G. and Murell, S.A.F. (1989). Permeability measurement techniques under hydrostatic and deviatoric stress conditions. *Rock at Great Depth, Maury & Fourmaintraux eds.*, Balkema, Rotterdam, 345-353.
- Rhett, D.W. and Teufel, L.W. (1992). Effect of reservoir stress path on compressibility and permeability of sandstones. *SPE*, paper 24756.
- Teufel, L.W. (1987). Permeability changes during shear deformation of fractured rock. *28th US Symposium on Rock Mechanics, Tucson*, 473-480.
- Walsh, J.B. (1981). Effect of pore pressure and confining pressure on fracture permeability. *Int.J.Rock Mech.Min.Sci & Geomech.Abstr*, vol.18, 429-435.
- Wilhelmi, B. and Somerton W.H. (1967). Simultaneous measurement of pore and elastic properties of rocks under triaxial conditions. *SPE Journal*, Sept., 283-294.
- Yale, D.P. (1984). Network modelling of flow, storage and deformation in porous rocks. *Stanford University Thesis*.
- Zhu, W. and Wong, T.F. (1997). The transition from brittle to cataclastic flow : permeability evolution. *Journal of Geophysical Research*, vol. 102, B2, Feb. 10, 3027-3041.